nature physics
SUPPLEMENTARY INFORMATION
DOI: 10.1038/NPHYS3465

Long-distance transport of magnon spin information in a magnetic insulator at room temperature

L.J. Cornelissen, J.Liu, R.A. Duine, J. Ben Youssef & B. J. van Wees

A. Comparison with local spin Hall magnetoresistance measurements

To study the limiting case $d \to 0$, we do a local spin Hall magnetoresistance (SMR) measurement[1] on the injector. In such a measurement, a current is sent through a platinum strip on a YIG film while simultaneously measuring the first harmonic voltage over that same strip. The resistance that is measured will depend on the orientation of the YIG magnetization $\boldsymbol{M}$ with respect to the spin orientation of the spin accumulation $\boldsymbol{\mu_s}$ in the platinum. When $\boldsymbol{M} \perp \boldsymbol{\mu_s}$, electron spins arriving at the Pt|YIG interface are absorbed. When $\boldsymbol{M} \parallel \boldsymbol{\mu_s}$, the spins are (mostly) reflected. This leads to a higher resistance for the perpendicular case than for the parallel case, and the difference in resistance $R^{SMR} = R_{\perp} - R_{\parallel}$ is the SMR response.

We do an SMR measurement on the injector strip of our devices. The sample is then rotated in an external field to extract the magnitude of the SMR response. We find $R_l^{SMR} = (6.8 \pm 0.2) \times 10^4\ \Omega/\mathrm{m}$ (averaged over 5 devices), approximately 57 times larger than the maximum non-local signal ($R_{nl}^{1\omega} = 1.2 \times 10^3\ \Omega/\mathrm{m}$, for $d = 200$ nm). Note that with an SMR measurement we measure the difference between the number of absorbed spins and reflected spins, while in the non-local geometry we are sensitive only to the number of spins that are transferred across the interface when $\boldsymbol{M} \parallel \boldsymbol{\mu_s}$. The magnitude of the SMR signal is governed by the spin conductance of the platinum strip[2] g_{Pt}, while the number of transferred spins for the collinear case is governed by the effective mixing conductance[3] $g_S \approx 0.16 g_r$, as well as the Pt spin conductance. In terms of spin resistances and in the diffusive regime, we can calculate the ratio of the non-

DOI: 10.1038/NPHYS3465

local signal and the SMR signal to be $R_{nl}/R^{SMR} = \frac{R^S_{Pt}}{2R^S_{Pt}+2R^S_i+R^S_{YIG}}$. Here, R^S_{Pt} is the spin resistance of the platinum, R^S_i the spin resistance due to the Pt|YIG interface and R^S_{YIG} the spin resistance of the YIG channel. The platinum spin conductance (limited by the spin diffusion length) is[2] $g_{Pt} \approx 10^{14}\,\Omega^{-1}m^{-2}$, while the effective mixing conductance of the Pt|YIG interface is $g_S \approx 10^{13}\,\Omega^{-1}\mathrm{m}^{-2}$. Using the Pt|YIG interface area of $A \approx 1.9\times10^{-12}\,\mathrm{m}^2$ and the ratio $R_{nl}/R^{SMR} = 1/57$, we find for the spin resistance of the YIG channel in the shortest distance non-local measurement $R^S_{YIG} \approx 0.2\,\Omega$. Given the channel dimensions of $L_C = d = 200$ nm, $w_C = 12.5\,\mu$m and $t_C = 200$ nm, this yields a YIG spin conductivity of $\sigma^S_{YIG} \approx 4\times10^5$ S/m. Interestingly, this spin conductivity is only one order of magnitude lower than the electrical conductivity of some common metals, for instance the platinum that we use, $\sigma_{Pt} = (2.1 \pm 0.2)\times10^6$ S/m. This underscores the fact that YIG is indeed an excellent conductor for magnon spin currents.

The symmetry of the SMR signal as a function of angle α is the same as that of the non-local resistance, since the SMR response also involves both the spin Hall effect and the inverse spin Hall effect, leading to the $\cos^2\alpha$ dependence. Furthermore, the signs of the local and non-local signal agree, which is required since both effects involve the square of the spin Hall angle in platinum. Note that the sign of the non-local signal as described theoretically by Zhang & Zhang[4] is opposite from the sign we observe. This is still consistent with our observations however, since the parallel layer geometry (Pt|YIG|Pt) described in their paper yields an opposite direction for the spin current entering the platinum detector compared to our planar non-local geometry.

B. Sign of the second harmonic response

As shown in the inset of figure 3b of the main text, the second harmonic signal changes sign for very short distances ($d = 200$ nm), while the signal is maximum for $d \approx 600$ nm. To investigate this sign change, we performed local measurements of the spin Seebeck voltage in the current heating configuration[5,6]. In this configuration, a charge current is applied to the injector and the second harmonic voltage over the injector is measured simultaneously. Figure S1 shows a comparison for the local (S1a), short distance non-local (S1c) and longer distance non-local (S1b, d) signals. It can be seen that the signal sign for the shortest distance matches that of the local spin Seebeck signal. We can understand this as when we move the detector closer and closer to the injector, we approach the limit of a local measurement. While it would be of great interest to develop a quantitative picture, this is outside the scope of this paper. Instead, we provide a qualitative explanation, guided by the fact that the change in sign occurs at a distance $d \approx 200$ nm which is comparable to the YIG film thickness $t_{YIG} = 200$ nm.

The second harmonic signal is due to thermally generated magnons, excited by the heat generated by Joule heating due to the current flowing in the injector strip. Since the heat conductivity of the GGG substrate is close to that of the YIG film, most of the heat generated in the injector will flow towards the substrate, normal to the plane of the film.

The spin Seebeck effect in Pt|YIG bilayers is well described as being driven by temperature differences at the Pt|YIG interface[7]. Additionally, a bulk spin Seebeck effect has been proposed where the driving force is the temperature gradient in the bulk of the YIG[8,9]. Following the bulk theory, an applied temperature gradient ∇T in a YIG film generates a magnon spin current parallel to ∇T. Since the YIG film thickness is much smaller than the magnon spin relaxation

DOI: 10.1038/NPHYS3465

length a magnon spin accumulation will build up at the interfaces, having opposite sign at the YIG|GGG compared to the Pt|YIG interface.

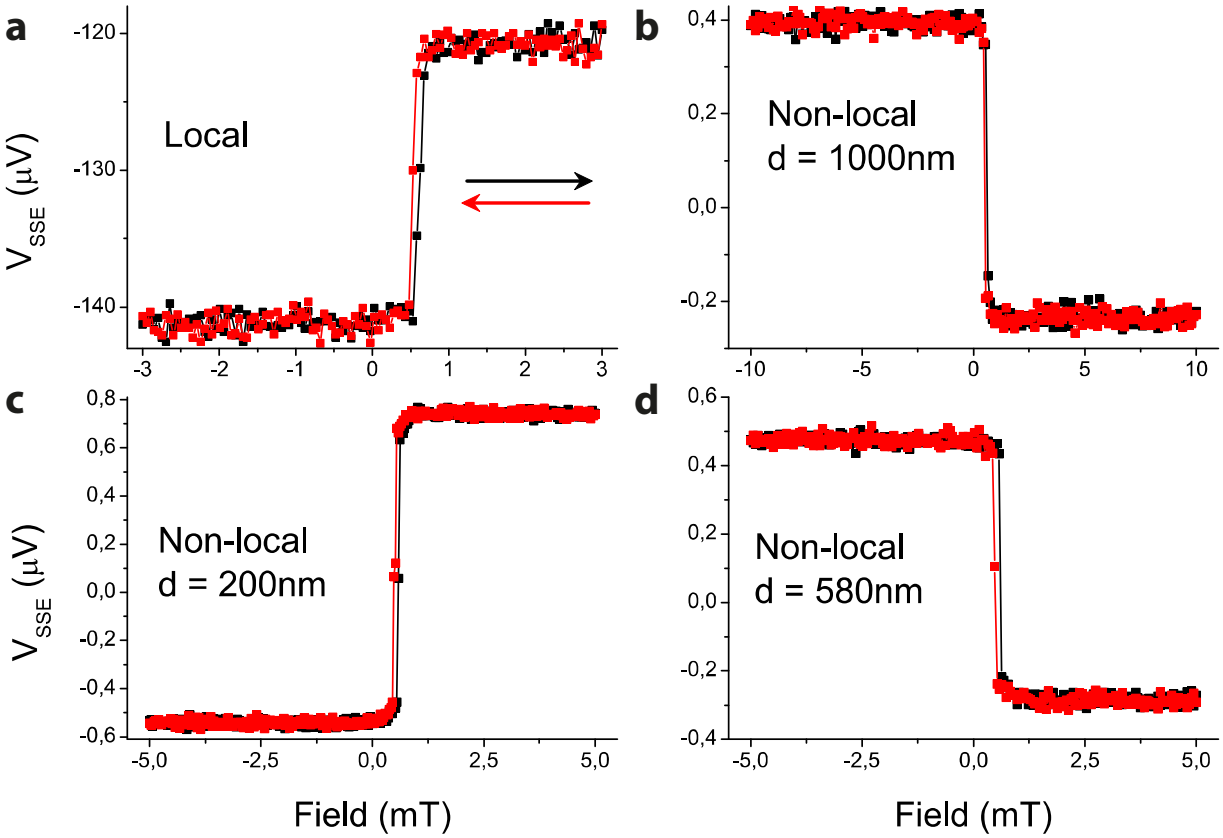

Figure S1: Comparison of the sign of the second harmonic signal. The spin Seebeck voltage V_{SSE} is measured as a function of the external field, for a fixed sample position. Due to the $\cos\alpha$ symmetry of V_{SSE}, we observe a difference in signal for positive ($\alpha = 0$) and negative ($\alpha = -180°$) fields. From figure a and c it is clear that sign of the local V_{SSE} agrees with that of the shortest non-local distance ($d = 200$ nm), while for longer distances (figures b and d) the sign is reversed. This can also be seen from the inset in figure 3b in the main text. In the local measurement in figure a, a large offset voltage is present which we believe is caused by the conventional Seebeck effect at the Pt|(Ti/Au) interfaces in the device. The small offset in the non-local measurements in figures b, c and d has the same origin, but is much smaller since only a fraction of the heat generated in the injector reaches the detector. For distances larger than a few microns, the offset vanishes completely.

For the situation where d is comparable to t_{YIG}, the magnon accumulation at the Pt|YIG interface dominates the signal, giving rise to an agreement in sign for the local and 200 nm non-local signal. For distances further away, diffusion of the YIG|GGG magnon accumulation across the film thickness compensates the Pt|YIG accumulation and becomes dominant for $d > t_{YIG}$, causing the sign reversal as a function of distance.

As a consequence, for distances $d < 500$ nm, the assumption that the injector is an ideal localized magnon source is no longer valid for the thermal generation case. Therefore, signal decay in this regime is no longer well described by equation 7 in the main text and we omitted the devices with $d < 500$ nm when fitting the second harmonic signal. Obtaining a quantitative picture of this behavior will require detailed modelling of the heat and spin currents in the sample.

DOI: 10.1038/NPHYS3465

References

1. Nakayama, H. *et al.* Spin Hall Magnetoresistance Induced by a Nonequilibrium Proximity Effect. *Phys. Rev. Lett.* **110,** 206601 (2013).

2. Castel, V., Vlietstra, N., Ben Youssef, J. & van Wees, B. J. Platinum thickness dependence of the inverse spin-Hall voltage from spin pumping in a hybrid yttrium iron garnet/platinum system. *Appl. Phys. Lett.* **101,** 132414 (2012).

3. Flipse, J. *et al.* Observation of the Spin Peltier Effect for Magnetic Insulators. *Phys. Rev. Lett.* **113,** 027601 (2014).

4. Zhang, S. S.-L. & Zhang, S. Spin convertance at magnetic interfaces. *Phys. Rev. B* **86,** 214424 (2012).

5. Vlietstra, N. *et al.* Simultaneous detection of the spin-Hall magnetoresistance and the spin-Seebeck effect in platinum and tantalum on yttrium iron garnet. *Phys. Rev. B* **90,** 174436 (2014).

6. Schreier, M. *et al.* Current heating induced spin Seebeck effect. *Appl. Phys. Lett.* **103,** 242404 (2013).

7. Xiao, J., Bauer, G. E. W., Uchida, K., Saitoh, E. & Maekawa, S. Theory of magnon-driven spin Seebeck effect. *Phys. Rev. B* **81,** 214418 (2010).

8. Rezende, S. M. *et al.* Magnon spin-current theory for the longitudinal spin-Seebeck effect. *Phys. Rev. B* **89,** 014416 (2014).

9. Hoffman, S., Sato, K. & Tserkovnyak, Y. Landau-Lifshitz theory of the longitudinal spin Seebeck effect. *Phys. Rev. B* **88,** 064408 (2013).